

Nano-pantography

NSF NIRT Grant DMI0303790

Vincent M. Donnelly, Demetre J. Economou, Paul Ruchhoeft

University of Houston

Sungho Jin

University of California, San Diego

1. Overview: Current focused ion beam techniques are capable of writing nanometer-sized features, but are very slow. The aim of this project is a novel, radically different approach to high-throughput and versatile fabrication of nanometer scale complex patterns over large areas. A broad area collimated beam of ions is directed at a silicon wafer, and focused as an orderly array of nanometer size spots with the use of sub-micron sized electrostatic lenses. Simulations indicate that regardless of the achievable resolution of current lithography, this method can improve resolution by a factor of up to 100. When the wafer is tilted off normal (with respect to the ion beam axis), the focal point is laterally displaced, allowing the focused beams to be rastered, thus forming any arbitrary pattern. This is the essence of nano-pantography. The desired pattern can be replicated simultaneously in perhaps billions of spots over tens of sq. cm. The initial stage of this project has focused on four aspects: a) Design, construction and assembly of the plasma beam system, b) simulations of focusing of ions in the microlenses, c) construction of the micro-Einzel lens arrays, and d) growth of carbon nanotubes by plasma enhanced CVD. Several significant milestones were achieved and are discussed below.

2. Plasma Reactor and Ion Beam: The plasma reactor consists of a custom multi-port stainless steel reactor, a target electrode (cathode), an ion acceleration ring electrode, and a grounded extraction grid. The target electrode is powered by a radio-frequency source (13.56 MHz). To achieve the minimum feature size (~ 1 nm) in the nanopantography process, the energy spread (ΔE) in the ion beam must be kept to a minimum. Since $\Delta E \approx T_e$, where T_e is the plasma electron temperature, it is important to obtain the minimum T_e . To obtain the low T_e needed, the discharge was modulated, as depicted in Fig. 1. T_e decays to less than 1 eV near the end of the OFF period without a large decay in the positive ion and nearly equal electron density. Near the end of the OFF period, a high positive voltage pulse is applied to the ring electrode (Fig. 1). When the OFF-period plasma experiences this condition, electrons swarm to the positive ring electrode and the plasma potential quickly reaches the ring potential (V_r). This unusual condition causes a potential of $-V_r$ to exist between the plasma and all grounded surfaces. Hence, positive ions are accelerated to the grounded grid and the majority of them pass through the grid and into the downstream region with an energy equal to V_r . Ions are rejected during the ON portion by applying a 100V pulse to a downstream rejection grid. Since charge-exchange collisions must be suppressed, differential pumping was used reduce the downstream pressure. Ion energy measurements were carried out at the bottom of the downstream chamber in the position where the substrate with the Einzel lens arrays will be positioned. A three-grid ion energy analyzer was constructed for this purpose. The first derivative (dn_i/dV) of the ion current vs. the second grid voltage is the ion energy distribution. A sample dn_i/dV vs V measurement is shown in Fig. 2 for the pulsed plasma with a constant DC bias, and the rejection grid filtering out the initial portion of the OFF cycle. The sharp peak in the latter trace, at a peak energy nearly equal to the voltage on the acceleration ring electrode confirms that the scheme for generating

mono-energetic ions is working. Our simulations indicate that these energy spreads are sufficiently narrow to achieve a high degree of focus at the bottoms of the lenses.

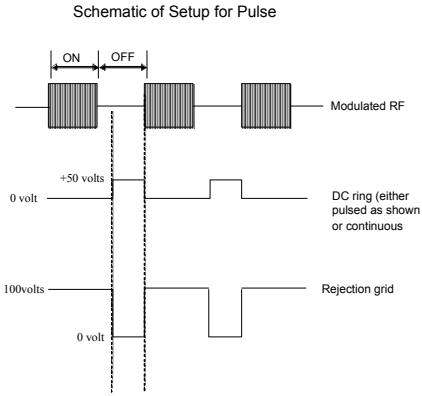


Fig. 1. Pulsing scheme for the plasma and ion beam.

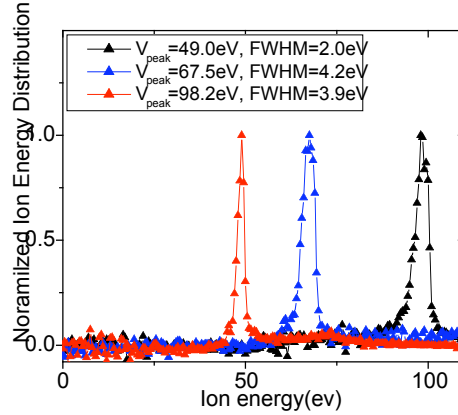


Fig. 2. Ion energy distributions for the pulsed plasma with and with selection by the rejection grid.

3. Einzel Lens Designs: Simulations were carried out for the Einzel lens geometry shown in Fig. 3. Ions exited the plasma through the grounded grid with an energy of 100 eV, drifted to the lens arrays and were decelerated by the potential on the top electrode on the lenses. Laplace's equation was solved for the axisymmetric symmetry of the individual Einzel lenses. For an optimized 500 nm dia. lens design, the micro-ion beams can be focused to a spot (FWHM) of 4.2 nm (Fig. 4), better than a 100-fold reduction in size, compared to the diameter of lens.

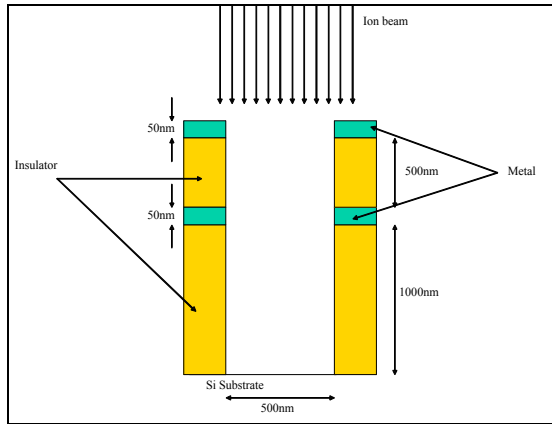


Fig. 3. Schematic of the Einzel lens design.

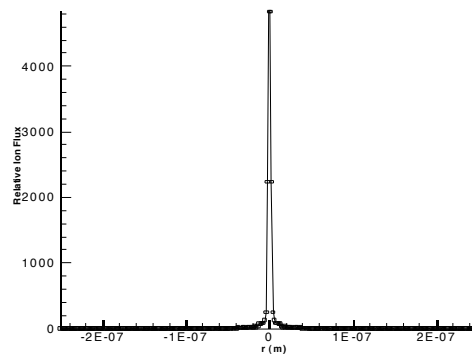


Fig. 4. Simulation of the ion flux at the bottom of the Einzel lens as a function of radial position.

To fabricate the large areas of lenses, we are employing ion beam aperture array lithography (AAL) to define an array of circular openings in resist that is etched through the conducting electrode material. In these initial studies, a single layer of metal was used, as opposed to the more complex two layers of metal in the lenses (Fig. 3) used in the simulations in Fig. 4. Additional simulations showed that this simpler lens structure could achieve nearly the same degree of ion focusing. The process flow for fabricating the lens structures is: (a) first, a silicon

wafer is spin-coated with 500nm of polyimide and a 50nm thick gold coating is sputtered onto the active regions of the substrate through a shadow mask. The entire substrate is then coated with 100nm thick silicon dioxide and 200nm of poly(methyl methacrylate) (PMMA). After lithography (b), the resist structures are etched through the silicon dioxide by CHF_3 reactive ion etching (RIE), through the gold by Ar sputter etching, and through the polyimide by O_2 RIE. As a final step, the oxide layer is stripped using hydrofluoric acid. Fig. 5 shows an SEM of the lens structure in PMMA resist. The pattern area is 0.36cm^2 .

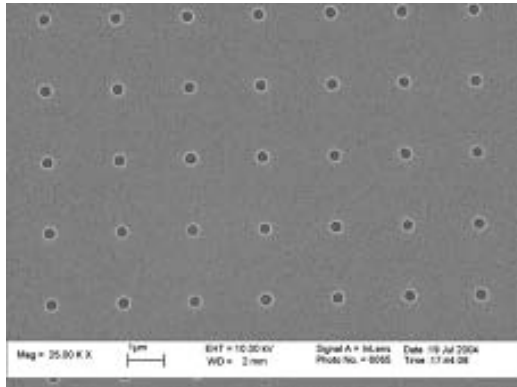


Fig. 5: SEM of the lens structures in PMMA resist.

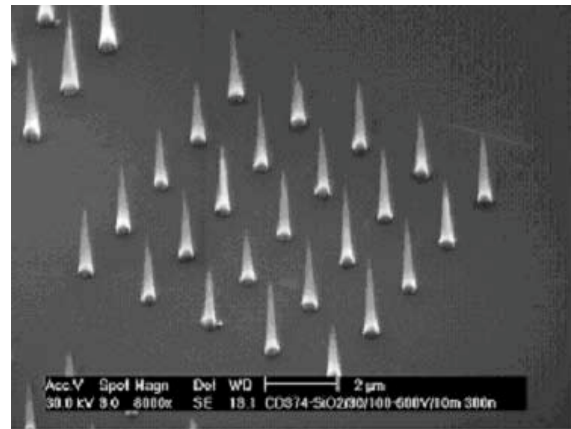


Fig. 6. Patterned and aligned carbon nanotubes.

4. Carbon Nanotube Growth: The nanopantography technique being developed will eventually be applied for fabrication of nanostructures. During the first year of the program, the following progress has been made at the University of California, San Diego in order to establish nanostructure fabrication methodology in preparation for the use of nanopantography. A microwave plasma CVD system and DC plasma CVD system have been constructed for growth of carbon nanotubes. Well-aligned, patterned and uniform carbon nanotubes have been grown, using nickel and iron catalyst particles. Excellent field emission properties have been obtained from these aligned nanotubes. Shown in Fig. 6 is a patterned nanotube array synthesized by using such patterned catalyst islands. Much finer-scale nanotubes with $\sim 5\text{-}10$ nm diameter were also fabricated using ~ 5 nm diameter catalyst particles obtained by chemical processing. A similar nanotube growth is expected when the catalyst islands are patterned using the nanopantography patterning process which is currently being developed. We have also carried out the field emission measurement for the vertically aligned MWNT samples prepared by microwave plasma enhanced CVD. Smooth and consistent I-V curves were obtained for the sample at various distances in steps of $3.3\ \mu\text{m}$ between anode probe and vertically aligned nanotubes. The emission current density values for the aligned nanotubes grown by microwave plasma CVD were typically in the range of $0.5\text{-}1.5\ \text{A}/\text{cm}^2$. The field emission behavior from the DC plasma aligned nanotubes was generally similar to that for the microwave plasma CVD sample.

5. Acknowledgements: We acknowledge support from NSF NIRT award DMI-0303790.

References

[1] For further information about this project email vmdonnelly@uh.edu